Original Article
ISSN (Online): 2582-7472

ShodhKosh: Journal of Visual and Performing Arts
July-December 2023 4(2), 5947–5957

HALL AND ION SLIP EFFECTS ON THE MHD CONVECTIVE FLOW FOR MIXED CONVECTION BOUNDARY LAYER FLOW OF A NANOFLUID ALONG AN INCLINED PLATE EMBEDDED IN A POROUS MEDIUM

N. Srinivasa Rao [1]

[1] Associate Professor, Department of Mathematics, GFGC, Kolar, Karnataka, India

ABSTRACT

In the present investigation, the radiative MHD flow of an incom- pressible viscous electrically conducting non-Newtonian nanofluidover an exponentially accelerated vertical porous surface has been considered. Under the influence of slip velocity in a rotating frame, it takes Hall and ion slip impacts into account. Water and ethylene glycol mixture is considered a base Casson fluid. A steady uniform magnetic field is applied under the postulation of a low magnetic Reynolds number. The ramped temperature and time-altering concentration at the surface are considered. First-order consistent chemical reaction and heat absorption are also regarded. Silver and Titania nanoparticles are disseminated in base fluid water and ethylene glycol combination should be formed by a hybrid nanofluid. The Laplace transformation technique is employed on the non-dimensional governing equations to ensure closed-form ana- lytical solutions. The graphical representations scrutinize the effects of physical parameters on significant flow characteristics. The temperature of Ag-TiO2/WEG nanofluid is relatively superior to that of Casson Ag-WEG nanofluid. Species concentra- tion of Casson hybrid Ag-TiO2/WEG nanofluid decreases with an increase in Schmidt number and chemical reaction parameters. The heat absorption increases the Nusselt number near the surface, while Ag and TiO2 nanoparticle volume fractions tend to lessen it.

Keywords: Hall Effect, Nano Fluid, Porous Medium, MHD, Mixed Convection

Corresponding Author

N. Srinivasa Rao,
n.s.s.rao2526@gmail.com

DOI
10.29121/shodhkosh.v4.i2.2023.6377

Funding: This research received no specific grant from any funding agency in the public, commercial, or not-for-profit sectors.

1. INTRODUCTION

The recent developments in technology require an innovative revolution in heat transfer. The research on nanofluids has been amplified fast. According to reports nanofluids are advantageous heat transport fluids for engineering and manufacturing applications. The heat transport development of nanofluids is principally reliant on the heat conductivity of nanoparticles, particles volume concentration and mass flow discharges. Under steady particles volume concentration and flow discharges, the heat transport development only on the heat conductivity of the nanoparticles. The heat conductivity of nanoparticles may be revised or transformed by developing hybrid nanoparticles. Hybrid nanoparticles are nanoparticles created by two or additional different substantial of nanometer scale. The fluids developed through hybrid nanoparticles of transformed metals interested in the base fluid are recognized as hybrid nanofluids.

A large effective diversity of applications is applied in contemporary science, technol- ogy and engineering territory, such as chemical manufacture, automobile, solar collector, nuclear reactor, industrial cooling, solar synthesis, gas sensing, bio-sensing, etc. The heat transfer of effective fluids may be improved using a variety of methods. One of these is to hang nanoparticles (Cu, CuO, Ag, Fe, Au, MgO, MoS2, Al, Al2O3, TiO2, etc.) by dimension among 1 and 100 nm to the base fluid (e.g. H2O, C2H6O2 (ethylene glycol), C2nH4n+2On+1 (polyethylene-glycol), glycerine, blood, engine oil, (C6H8O6)n (sodium alginate), . . . etc.).A nanofluid describes a liquid that contains nanometer-sized particles known as nanoparticles. These fluids are nanoparticle colloidal suspensions in a base fluid. Metallic (Al, Cu), oxides (Al2O3, CuO, TiO2, SiO2), carbohydrates (SiC), nitrides (AlN, SiN), or nonmetallic substances (graphite, silicon nanotubes) are commonly employed in nanofluids, and the base fluid is generally a conductive fluid, like example water or ethyl glycol. Nanofluids have unique features that make them potentially helpful in a wide range of heat transfer applications, such microelectronics, fuel cells, pharmacological operations, and hybrid-powered engines. They have higher thermal conductivity and convective heat transfer coefficients than the base fluid. Practical investigations . This to improve the constructive thermal characteristics of nanofluids and circumvent dis- crepancies in the traditional nanofluids. Realistic implementations of these concepts were first conceded by Choi [1] to enhance the heat conductivity and speed of heat transport. Demonstrate that average thermal conductivity gains are in the range of 15-40% beyond its base fluid, and heat transfer coefficient upsurges are up to 40%. The improvement in performance was ascribed to Brownian motion, thermophoresis, particle shape/surface area, temperature, and liquid layering on the nanoparticle-liquid interface. Several writers addressed, demonstrating why natural convection heat transfer is characterised not only by the effective thermal conductivity of the nanofluid, but also by the susceptibility to the viscosity model, which plays a significant role in heat transfer behaviour [2-11].

Sundar et al. [12] discussed that hybrid nanofluids are additional effectual heat transport fluids than solitary nanoparticle-based nanofluids or traditional fluids. Sarkar et al. [13] opined that appropriate hybridizations may create hybrid nanofluids extremely promis- ing for heat transport development; nevertheless, more investigative works are required in development and immovability, characterizations and applications to defeat the dis- putes or challenges. Devi et al. [14] explored the magnetohydrodynamic (MHD) flow of Cu-Al2O3/water hybrid nanofluids. Oxide nanoparticles have a lesser amount of heat con- ductivity than metallic nanoparticles. A superior volume fraction of oxide nanoparticles are required to have the needed heat effectiveness. The computational outcomes indicate that heat replaced the speed of Cupper-alumina/water hybrid nanofluids is more signifi- cant than that of the Cu□H2O nanofluids. The characteristics of hybrid nanofluids, based on different kinds of metallic and oxides, such as MgO, Fe3O4, Silver, copper oxide, Copper, and MWCNTs, have been demonstrated by Minea [15]. This showed most excellent viscos- ity amplification for CuO-Cu hybrid nanoparticles. Toghraie et al. [16] illustrated a variety of correlations for heat conductivities of nanofluids cleared by preceding researchers. They recommended an innovative correlation for the heat conductivity of ZnO-Titania/Ethylene Glycol hybrid nanofluids by highest accurateness using investigational findings. Hayat et al.[17] explored the three-dimensional Brinkman hybrid nanofluids models to examine the heat transport features of copper oxide/H2O and Silver□CuO/H2O nanofluids past a lin- early stretching surface with heat radiation and homogeneous and heterogeneous reactive flows. An exhaustive and narrative review on heat transport investigation of predictable and hybrid nanofluids by the non-Newtonian fluid model was determined by Jamshed et al.[18] and Ellahi [19]. Aman et al. [20] exhibited the sodium alginate-based hybrid nanofluids (Copper-Alumina) flow in vertical ducts. Usman et al. [21] discussed the nonlinear thermal radiation and time-dependent heat conductivity due to rotating flow alumina-H2O hybrid nanofluids past a stretching sheet with a magnetic field and buoyancy force.

Despite the complications of producing non-Newtonian fluids, applied mathematicians and engineers are engaged in non-Newtonian fluid mechanics. Because the flow and heat transport features of those fluids are significant to numerous and miscellaneous systems in biotechnology, pharmaceutical and chemical engineering, etc. Non-Newtonian model- ing has a nonlinear relationship with the stress and rate of strain. The mechanical features of non-Newtonian fluids, and hear thin or shear thickness, usual stress difference, and visco-elastic reaction, may not be portrayed through the conservative theories; hence, an innovative and effectual prediction is required. Various constitutive equations portray the movement and heat transport mechanism, along with these; the Casson model has grown a great deal of acceptance. Casson fluid model becomes a non-Newtonian fluid to the investi- gators due to its wide-range applications in biomedical and industrial engineering, energy production, geophysical fluid mechanics and dynamics. Among plentiful non-Newtonian models, [22] influenced Hall electromotive forces on the pump flow of viscous fluid through a porous medium in an unsymmetrical vertical conduit. Koumy et al. [23] scrutinized iden- tically taking Maxwell fluid toward

deliberation. The performances of learning reveal that the average speed dispensation accentuates through elevated ethics of Hall parameteri- zation. Motsa and Shateyi [24] deliberated the results of Hall and ion slip for the flow of MHD micropolar fluid past the flat surface. Hall and ion slip impacts on peristaltic flow and heat transport inquiry by ohmic heating were explored by Asghar et al. [25]. Krishna and Chamkha [26] examined the MHD natural convective rotating flow of nanofluids through a semi-infinite porous moving surface. Krishna et al. [27] addressed the MHD convective flow of squeezing viscous fluid through a never-ending vertical porous surface taking Hall impacts into account. Hall and ion slip effects on unsteady MHD convective rotating flow of nanofluids were discussed by Krishna and Chamkha [28]. Krishna [29] investigated the heat transport on the steady MHD flow of copper and alumina nanofluids past a stretching porous surface. Krishna et al. [30] investigated the Hall and ion slip effects on the unsteady MHD free convective rotating flow through the porous medium past an exponentially accel- erated inclined plate. The combined effects of Hall and ion slips on the MHD rotating flow of ciliary propulsion of microscopic organisms through the porous medium were studied by Krishna et al. [31]. Krishna and Chamkha [32] investigated the Hall and ion slip effects on the MHD convective flow of an elastico-viscous fluid through the porous medium between two rigidly rotating parallel plates with time fluctuating sinusoidal pressure gradient. Krishna [33] reported the Hall and ion slip effects on MHD free convective rotating flow bounded.

2. FORMULATION OF THE PROBLEM

Under these assumptions, the governing equations that describe the physical situation in a rotating frame are specified by,

$$\frac{\partial u}{\partial x}+\frac{\partial v}{\partial y}=0 \tag{1}$$

$$\frac{\partial u}{\partial t}+w\frac{\partial u}{\partial z}-2\Omega v=v\frac{\partial^2 u}{\partial z^2}+\frac{B_0 J_y}{\rho}-\frac{v}{k}u+g\beta(T-T_\infty)+g\beta^*(C-C_\infty) \tag{2}$$

$$\frac{\partial v}{\partial t}+w\frac{\partial v}{\partial z}+2\Omega u=v\frac{\partial^2 u}{\partial z^2}-\frac{B_0 J_x}{\rho}-\frac{v}{k}v \tag{3}$$

$$\frac{\partial T}{\partial t}+w\frac{\partial T}{\partial z}=\frac{k_1}{\rho C_p}\frac{\partial^2 T}{\partial z^2}-\frac{Q_0}{\rho C_p}(T-T_\infty)+Q_l^*(C-C_\infty) \tag{4}$$

$$\frac{\partial C}{\partial t}+w\frac{\partial C}{\partial z}=D\frac{\partial^2 C}{\partial z^2}-K_l(C-C_\infty) \tag{5}$$

The magnetic and viscous dissipations are neglected in this study. The third and fourth terms on the right-hand side of the momentum Eq. (2) denote the thermal and concentration buoyancy effects, respectively. Also, the second and third terms on the right-hand side of the energy Eq. (4) represents the heat and radiation absorption effects, respectively. It is assumed that the permeable plate moves with a variable velocity in the direction of fluid flow. In addition, it is assumed that the temperature and the concentration at the wall as well as the suction velocity are exponentially varying with time. Under these assumptions, the suitable boundary conditions for the velocity, temperature and concentration fields are

$$u=u_0, v=0, T=T_w+\varepsilon(T_w-T_\infty)e^{nt}, \tag{6}$$

$$C=C_w+\varepsilon(C_w-C_\infty)e^{nt}, \text{at } z=0, \tag{7}$$

$$u=0, v=0, T\to T_\infty, C\to C_\infty, \text{at} z\to\infty \tag{8}$$

It is clear from Eq. (1) that the suction velocity at the plate surface is not a function of but a function of time only. Assuming that it takes the following exponential form as,

$$w = -w_0(1 + \varepsilon A e^{nt}) \tag{9}$$

where is a real positive constant, and are small less than unity, and is a suction velocity scale, which has non-zero positive constant. The negative sign indicates that suction is towards porous materials.

The electron-atom collision frequency is assumed to be very high, so that Hall and ion slip currents cannot be neglected. Hence, the Hall and ion slip currents give rise to the velocity in -direction. When the strength of the magnetic field is very large, the generalized Ohm's law is modified to include the Hall and ion slip effect

$$J = \sigma(E + V \times B) - \frac{\omega_e \tau_e}{B_0}(J \times B) + \frac{\omega_e \tau_e \beta_i}{B_0^2}((J \times B) \times B)\Big) \tag{10}$$

Additionally, it is assumed that the Hall parameter $\beta_e = \omega_e \tau_e \sim O(1)$ and the ion slip parameter,

$$\beta_i = \omega_i \tau_i << 1,$$

$$(1 + \beta_i \beta_e) J_x + \beta_e J_y = \sigma B_0 v \tag{11}$$

$$(1 + \beta_i \beta_e) J_y - \beta_e J_x = -\sigma B_0 u \tag{12}$$

Solving the Eqs. (10) and (11) we obtained as,

$$J_x = \sigma B_0(\alpha_2 u + \alpha_1 v) \tag{13}$$

$$J_y = -\sigma B_0(\alpha_2 v - \alpha_1 u) \tag{14}$$

where, $\alpha_1 = \frac{1+\beta_e\beta_i}{(1+\beta_e\beta_i)^2+\beta_e^2}$ and $\alpha_2 = \frac{\beta_e}{(1+\beta_e\beta_i)^2+\beta_e^2}$

Substituting the Eqs. (12) and (13) in (3) and (2) accordingly, it is acquired as,

$$\frac{\partial u}{\partial t} - w_0(1 + \varepsilon A e^{nt})\frac{\partial u}{\partial z} - 2\Omega v = v\frac{\partial^2 u}{\partial z^2} + \frac{\sigma B_0^2(\alpha_2 v - \alpha_1 u)}{\rho} - \frac{v}{k}u + g\beta(T - T_\infty) + g\beta^*(C - C_\infty) \tag{15}$$

$\frac{\partial v}{\partial t} - w_0(1 + \varepsilon A e^{nt})\frac{\partial v}{\partial z} + 2\Omega u = v\frac{\partial^2 v}{\partial z^2} - \frac{\sigma B_0^2(\alpha_2 u + \alpha_1 v)}{\rho} - \frac{v}{k}v$ as,

$$\frac{\partial q}{\partial t} - w_0(1 + \varepsilon A e^{nt})\frac{\partial q}{\partial z} + 2i\Omega q = v\frac{\partial^2 q}{\partial z^2} - \left(\frac{\sigma B_0^2(\alpha_1 + i\alpha_2)}{\rho} + \frac{v}{k}\right)q, + g\beta(T - T_\infty) + g\beta^*(C - C_\infty) \tag{16}$$

On introducing the non-dimensional quantities,

$$z^* = \frac{zw_0}{v}, q = \frac{q}{q_0}, t^* = \frac{tw_0^*}{v}, u_0^* = \frac{u_0}{w_0}, \theta = \frac{T-T_\infty}{T_w-T_\infty},$$

$$\phi = \frac{C-C_\infty}{C_w-C_\infty}, P_r = \frac{\mu c_p}{k_1}, Sc = \frac{v}{D},$$

$$Gr = \frac{g\beta v(T_w-T_\infty)}{w_0^3}, Gm = \frac{g\beta^* v(C_w-C_\infty)}{w_0^3}, K = \frac{v}{kw_0^2}, R = \frac{\Omega v}{w_0^2}, Kc = \frac{K_l v}{w_0^2},$$

$$M^2 = \frac{\sigma B_0^2 v}{\rho w_0^2}, H = \frac{Q_0 v}{\rho c_p w_0^2}, Q_l = \frac{v Q_l^*(C_w - C_\infty)}{(T_w - T_\infty)w_0^2}$$

Making use of the above non-dimensional variables, the governing Eqs. (4), (5) and (16) can be expressed in non-dimensional form as,

$$\frac{\partial q}{\partial t} - (1 + \varepsilon A e^{nt})\frac{\partial q}{\partial z} = \frac{\partial^2 q}{\partial z^2} - \left(M^2(\alpha_1 + i\alpha_2) + 2iR + \frac{1}{K}\right)q + Gr\theta + Gm\phi \quad (17)$$

$$\frac{\partial \theta}{\partial t} - (1 + \varepsilon A e^{nt})\frac{\partial \theta}{\partial z} = \frac{1}{\Pr}\frac{\partial^2 \theta}{\partial z^2} - H\theta + Q_l\phi \quad (18)$$

$$\frac{\partial \phi}{\partial t} - (1 + \varepsilon A e^{nt})\frac{\partial \phi}{\partial z} = \frac{1}{Sc}\frac{\partial^2 \phi}{\partial z^2} - Kc\phi \quad (19)$$

The boundary conditions are

$$q = u_0, \theta = 1 + \varepsilon e^{nt}, \phi = 1 + \varepsilon e^{nt} \text{ at } z = 0, \quad (20)$$

$$q \to 0, \theta \to 0, \phi \to 0 \text{ at } z \to \infty \quad (21)$$

To determine the solutions of the Eqs. (17)-(19) subjected to the boundary conditions (20) and (21). The Eqs. (17)-(19) represent a set of partial differential equations that cannot be solved in closed form. However, it can be reduced to a set of ordinary differential equations in dimensionless form that can be solved analytically. This can be done by representing the velocity, temperature and the concentration as,

$$q(z,t) = q_0(z) + \varepsilon e^{nt} q_1(z) + O(\varepsilon^2) \quad (22)$$

$$\theta(z,t) = \theta_0(z) + \varepsilon e^{nt} \theta_1(z) + O(\varepsilon^2) \quad (23)$$

$$\phi(z,t) = \phi_0(z) + \varepsilon e^{nt} \phi_1(z) + O(\varepsilon^2) \quad (24)$$

Substituting the Eqs. (22)-(24) into the Eqs. (17)-(19), equating the harmonic and non-harmonic terms, and neglecting the higher order powers of , and simplifying, it is obtained the following pairs of equations of zeroth and first orders be,

$$\frac{d^2 q_0}{dz^2} + \frac{dq_0}{dz} - \left(M^2(\alpha_1 + i\alpha_2) + 2iR + \frac{1}{K}\right)q_0 = -Gr\theta_0 + Gm\phi_0 \quad (25)$$

$$\frac{d^2\theta_0}{dz^2} + \Pr\frac{d\theta_0}{dz} - \Pr Hq_0 = -Q_l \Pr \phi_0 \quad (26)$$

$$\frac{d^2\phi_0}{dz^2} + Sc\frac{d\phi_0}{dz} - ScKc\phi_0 = 0 \quad (27)$$

Subjected to the boundary conditions

$$q_0 = u_0, \theta_0 = 1, \phi_0 = 1 \text{at } z = 0, \quad (28)$$

$$q_0 \to 0, \theta_0 \to 0, \phi_0 \to 0 \text{at } z \to \infty \quad (29)$$

Shear stress and the local surface heat transfer
These are defined by

$$\tau_w = \mu\left(\frac{\partial q}{\partial z}\right)_{z=0} = \rho w_0^2 q'(0)$$

Consequently, the local friction factor C_f is given by

$$C_f = \frac{\tau_w}{\rho w_0^2} = q'(0) = -m_1 a_2 - m_2 a_3 - m_3 a_4 - \varepsilon e^{nt}(m_1 a_{10} + m_2 a_{11} + m_3 a_{12} + m_4 a_{13} + m_5 a_{14} + m_6 a_{15})$$

3. THE LOCAL SURFACE HEAT FLUX IS GIVEN BY,

$$q_w = -k_2\left(\frac{\partial T}{\partial z}\right)_{z=0}$$

where, k_2 is the effective thermal conductivity, together with the definition of the local

4. NUSSELT NUMBER,

$$Nu_x = \frac{q_w}{T_w - T_\infty}\frac{x}{k_2}$$

It is written be,

$$\frac{Nu}{Re_x} = -\left(\frac{\partial\theta}{\partial z}\right)_{z=0} = m_2 + a_1(m_1 - m_2) + \varepsilon e^{nt}(m_1 a_6 + m_2 a_7 + m_4 a_8 + m_5 a_9)$$

where, $\mathrm{Re}_x = w_0 x/v$ is the local Reynolds number.

The local surface mass flux is given by, $q_m = -D_m \left(\frac{\partial C}{\partial z}\right)_{z=0}$

where D_m is the effective molecular diffusivity, together with the definition of the local Sherwood number, $S_x = q_m x/[D_m(C_w - C_\infty)]$

It is written be, $\frac{Sh}{Re_x} = -\left(\frac{\partial \phi}{\partial z}\right)_{z=0} = m_1 + \varepsilon e^{nt}\left(m_4 - a_5(m_1 - m_4)\right)$

5. DISCUSSION OF THE NUMERICAL RESULTS

Figures 1 and 2 show that, for the nanofluids Ag-WEG and Ag-TiO2/WEG and the ramped wall temperature and uniform wall temperature, the primary velocity component u increases on an increase in Hall and ion slip parameters βe and βi, while the magnitude of second velocity component v augments on an increase in Hall and ion slip parameters throughout the fluid medium. It was obvious that strengthening in the Hall parameter and ion slip parameter enhanced the resulting velocity and the momentum boundary layer thickness throughout the fluid medium. The inclusion of Hall parameters reduces the effec- tive conductivity and consequently moves down the magnetic renitent ferocity. In addition, the proficient conductance increases the ion slip parameter. For that motive, the attenua- tion forces decrease; as a result, velocity intensifies..Figures 3 exemplifies the impacts of φ1 and φ2 volume fractions of Ag and TiO2, respec- tively, on the primary and secondary velocities of nanofluids Ag-WEG and Ag-TiO2/WEG and both ramped wall temperature and uniform wall temperature. In the ramped wall tem- perature, the velocity u reduces, and v increases with enhancement volume fractions φ1 and φ2 and reversal behavior is observed for the kind of uniform wall temperature throughout the fluid medium. Therefore, the resultant velocity and thickness of the momentum bound- ary layer are increased for the ramped wall temperature and reduced for the uniform wall temperature with an increase in volume fractions of Ag and TiO2 in the entire fluid region. The numerical values of nanofluids Ag-WEG and Ag-TiO2/WEG on temperature θ , com- puted from the analytical solutions are displayed graphically in Figures 4 and 5 for various quantities of heat source parameters Q, volume fractions of Ag and TiO2 and time t. It is apparent from Figure 4 that fluid temperature and the thickness of the ther- mal boundary layer decrease on an enhancing heat source parameter for the ramped wall temperature and uniform wall temperature. The thermal border layer thickness for Casson hybrid nanofluid (Ag-TiO2) is superior to the Casson nanofluid (Ag-WEG). The heat resource parameter Q emerging in the energy equation quantified the amount of heat absorption per unit volume; it is known through Q0(T – T∞), Q0 being a heat source coefficient. This may be engaged either optimistic or pessimistic. The resource term represented the heat absorption for Q > 0 and heat generation if Q < 0. The growing values of heat absorption lessen the fluid temperature. High heat absorption Q.

Figure 1

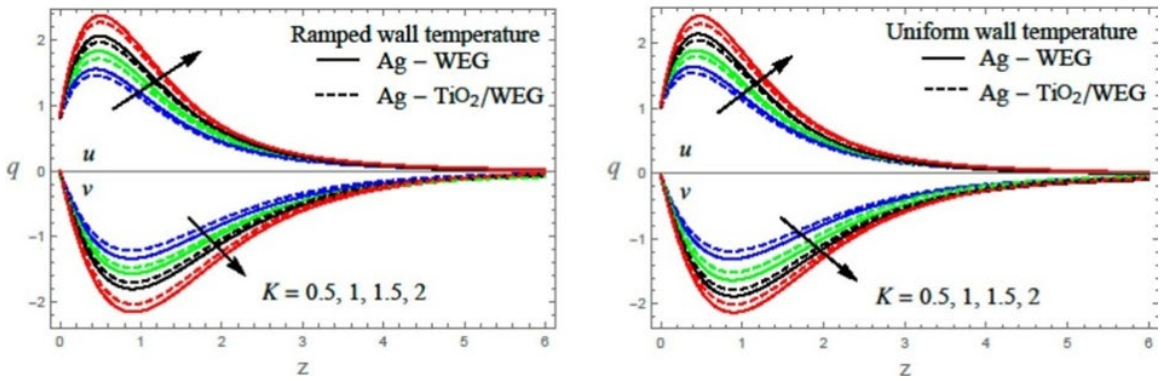

Figure 1 The Velocity Profiles Against Be.

Figure 2

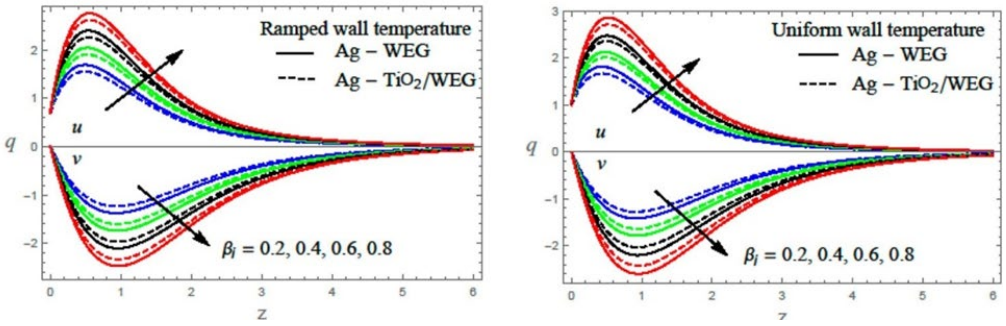

Figure 2 The Velocity Profiles Against Bi.

Figure 3

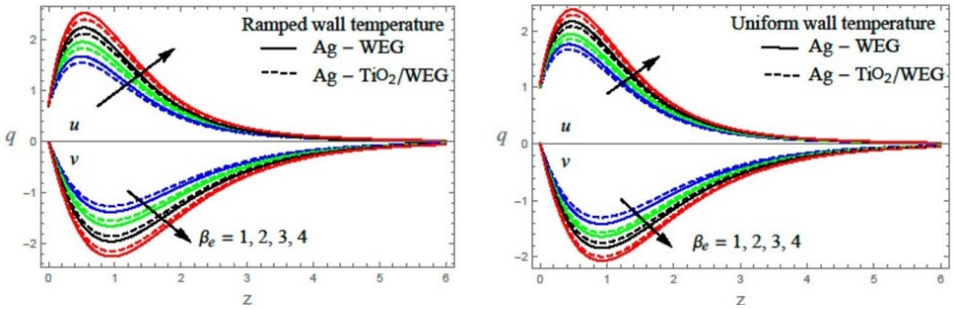

Figure 3 The Velocity Profiles Against Φ1 and Φ2.

Figure 4

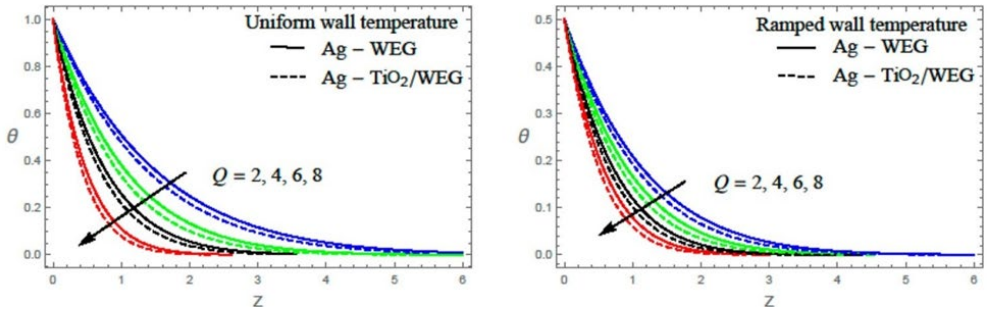

Figure 4 The Temperature Profiles Against Q.

Figure 5

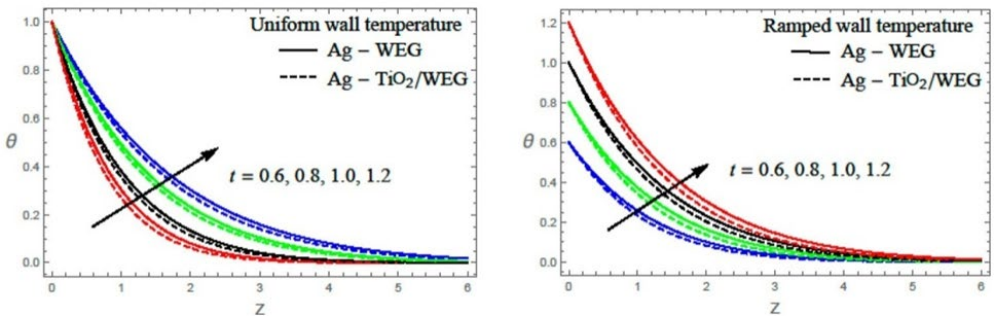

Figure 5 The Temperature Profiles Against t.

diminished the heat of the hybrid nanofluids. Hence, heat source or sink may be developed in material dispensation classifica- tion in theoretical research in material sciences. This behavior is expected since including silver nanoparticles to the base fluid or titania nanofluid or hybrid suspensions. The thermal conductivities of resultant fluid are increased. Hence, the hybrid suspensions had a high thermal capacity than nanofluids and a predictable one is purely Casson fluid. Accordingly, the high thermal conductance has a constructive consequence of enhancing the fluid temperature. The behavior of mono or hybrid nanofluids may be useful in the polymer dispensation system. As shown in Figure 5 the fluid temperature boosts with an increase in a specific instant of time. In addition, one may conclude that the temperature of a hybrid nanofluid (Ag-TiO2/WEG) is higher compared to that of a Casson nanofluid (Ag- WEG). It is observed and suggested that the utilization of hybrid composite nanoparticles as coolants or heaters in thermal engineering shows comparatively best strategies

The data in Table.1 show that variations in the Prandtl number Pr, the Brownian motion parameter Nb, and the buoyancy parameter Nb impact the lowered Nusselt(Nur) and Sherwood numbers(Shr) when the other parameters are held constant at the levels shown in the table header. The lowered Nur and reduced Shr rise with Pr for all combinations of Nb and Nr. With a constant Pr, the decreased Nur and the diminished Shr both drop as Nb and Nr grow. the ways in which modifications to the Lewis effect the decreased Nusselt number and the diminished Sherwood number. The lowered Nusselt number grows somewhat as the Lewis number upsurges, whereas the diminished Sherwood number upsurges significantly. include data regarding the flow's heat and mass transport characteristics in a manner suitable for study and mathematical calculations in engineering.

Table 1 Variation of Nur and Shr with Le,Nb and Nr for Nt=0.1, Nc=10 and Le = 10

Nb	Nr	Le=1			Le=5	Le=10	
		Nur	Shr	Nur	Shr	Nur	Shr
0.1	0.1	0.3892	0.2829	0.3839	0.8892	0.3923	1.0826
	0.2	0.3612	0.2797	0.3753	0.8856	0.3663	1.0457
	0.3	0.3332	0.2765	0.3667	0.8823	0.3403	1.0088
	0.4	0.3052	0.2733	0.3581	0.8787	0.3143	1.00857
	0.5	0.2772	0.2701	0.3495	0.8751	0.2883	1.00834
	0.6	0.2492	0.1289	0.3409	0.8715	0.2623	1.00811
	0.7	0.2212	0.1236	0.3323	0.8679	0.2363	1.00788
	0.8	0.2232	0.1235	0.3237	0.8643	0.2103	1.00765
0.3	0.1	0.2252	0.4253	0.3151	0.8607	0.1983	1.00742
	0.2	0.2272	0.4023	0.3065	0.8571	0.1863	1.00719
	0.3	0.2292	0.3793	0.2979	0.8535	0.1743	1.00696
	0.4	0.2312	0.3563	0.2893	0.8499	0.1623	1.00673
	0.5	0.2332	0.3333	0.2807	0.8463	0.1503	1.0065
	0.6	0.2352	0.3103	0.2721	0.8427	0.1383	1.00627
	0.7	0.2372	0.2873	0.2635	0.8391	0.1263	1.00604
	0.8	0.2392	0.2643	0.2549	0.8355	0.1143	1.00581
0.5	0.1	0.2412	0.2413	0.2463	0.8319	0.1023	1.00558
	0.2	0.2432	0.2183	0.2377	0.8283	0.1183	1.00535
	0.3	0.2452	0.1953	0.2291	0.8247	0.1234	1.00512
	0.4	0.2472	0.1723	0.2205	0.8211	0.1284	1.00489
	0.5	0.2492	0.1493	0.2119	0.8175	0.1236	1.00466
	0.6	0.2512	0.1263	0.2033	0.8139	0.1189	1.00443
	0.7	0.2532	0.1033	0.1947	0.8103	0.1235	1.0042
	0.8	0.2552	0.1233	0.1861	0.8067	0.1247	1.00397

CONFLICT OF INTERESTS

None.

ACKNOWLEDGMENTS

None.

REFERENCES

D.M. Yu, J.L. Routbort, S. Choi, Review and comparison of nanofluid thermal conductivity and heat transfer enhancements, Heat Transfer Eng. 29 (2008) 432–460.

S. Choi, Enhancing thermal conductivity of fluids with nanoparticles, in: D.A. Siginer, H.P. Wang (Eds.), in: Developments and Applications of NonNewtonian Flows, FED-Vol. 231, MD-Vol. 66, ASME, 1995, pp. 99–105.

H. Masuda, A. Ebata, K. Teramae, N. Hishinuma, Alteration of thermal conductivity and viscosity of liquid by dispersing ultra-fine particles, Netsu Bussei (Japan) 7 (4) (1993) 227–233.

J. Buongiorno, Convective transport in nanofluids, ASME J. Heat Transfer 128 (2006) 240–250.

S.K. Das, S. Choi, W. Yu, T. Pradeep, Nanofluids: Science and Technology, Wiley Interscience, New Jersey, 2007.

J. Eastman, S.U.S. Choi, S. Lib, W. Yu, L.J. Thompson, Anomalously increased effective thermal conductivities of ethylene-glycol-based nanofluids containing copper nanoparticles, Appl. Phys. Lett. 78 (6) (2001) 718–720.

J. Buongiorno, W. Hu, Nanofluid coolants for advanced nuclear power plants, in: paper no. 5705, Proc. ICAPP ’05, Seoul, May 15–19, 2005.

A.V. Kuznetsov, D.A. Nield, Natural convection boundary-layer of a nanofluid past a vertical plate, Int. J. Therm. Sci. 49 (2010) 243–247.

D.A. Nield, A.V. Kuznetsov, The Cheng-Minkowycz problem for natural convection boundary-layer flow in a porous medium saturated by a nanofluid, Int. J. Heat Mass Transfer 52 (2009) 5792–5795.

P. Cheng, W.J. Minkowycz, Free convection about a vertical flat plate embedded in a porous medium with application to heat transfer from a dike, J. Geophys. Res. 82 (1977) 2040–2044.

W.A. Khan, I. Pop, Boundary-layer flow of a nanofluid past a stretching sheet, Int. J. Heat Mass Transfer 53 (2010) 2477–2483

Sundar LS, Sharma KV, Singh MK, et al. Hybrid nanofluids preparation, thermal properties, heat transfer and friction factor – a review. Renew Sustain Energy Rev. 2017;68:185–198. doi:10.1016/j.rser.2016.09.108.

Sarkar J, Ghosh P, Adil A. A review on hybrid nanofluids: recent research, development and applications. Renew Sustain Energy Rev. 2015;43:164–177. doi:10.1016/j.rser.2014.11.023.

Devi SPA, Devi SSU. Numerical investigation of hydromagnetic hybrid Cu-Al2O3/water nanofluid flow over a permeable stretching sheet with suction. Int J Nonlin Sci Num Simul. 2016;17:249–257. doi:10.1515/ijnsns-2016-0037.

Minea AA. Challenges in hybrid nanofluids behavior in turbulent flow: recent research and numerical comparison. Renew Sustain Energy Rev. 2017;71:426–434.

Toghraie D, Vahid AC, Masoud A. Measurement of thermal conductivity of ZnO–TiO2/EG hybrid nanofluid. J Thermal Anal Cal. 2016;125:527–535.

Hayat T, Nadeem S. Heat transfer enhancement with Ag–CuO/water hybrid nanofluid. Results Phys 2017;7:2317–2324.

Jamshed W, Aziz A. A comparative entropy based analysis of Cu and Fe3O4/methanol Powell-Eyering nanofluid in solar thermal collectors subjected to thermal radiation, vari- able thermal conductivity and impact of different nanoparticles shape. Results Phys. 2018;9: 195–205.

Ellahi R. Special issue on recent developments of nanofluids. Appl Sci. 2018;8:192.

Aman S, Zokri SM, Ismail Z, et al. Effect of MHD and porosity on exact solutions and flow of a hybrid Casson-nanofluid. J Adv Res Fluid Mech Therm Sci. 2018;44:131–139.

Usman M, Hamid M, Zubair T, et al. Cu-Al2O3/water hybrid nanofluid through a permeable sur- face in the presence of nonlinear radiation and variable thermal conductivity via LSM. Int J Heat Mass Transf. 2018;126:1347–1356.

Abo-Eldahab E, Barakat E, Nowar K. Hall currents and heat transfer effects on peristaltic transport in a vertical asymmetric channel through a porous medium. Math Prob Eng. 2012;2012:840203. doi:10.1155/2012/840203.

Koumy SRE, Barakat ESI, Abdelsalam SI. Hall and porous boundaries effects on peristaltic trans- port through porous medium of a Maxwell model. Transp Porous Media. 2012;94:643–658.

Motsa SS, Shateyi S. The effects of chemical reaction, Hall and ion-slip currents on MHD micropo- lar fluid flow with thermal diffusivity using a novel numerical technique. J Appl Math. 2012: 1–30. doi:10.1155/2012/689015.

Asghar S, Hussain Q, Hayat T, et al. Hall and ion slip effects on peristaltic flow and heat transfer analysis with Ohmic heating. Appl Math Mech. 2014;35:1509–1524.
Krishna MV, Chamkha AJ. Hall and ion slip effects on MHD rotating boundary layer flow of nanofluid past an infinite vertical plate embedded in a porous medium. Results Phys. 2019;15:102652. doi:10.1016/j.rinp.2019.102652.
Krishna MV, Swarnalathamma BV, Chamkha AJ, et al. Joule and Hall effects on MHD rotating mixed convective flow past an infinite vertical porous plate. J Ocean Eng Sci. 2019;4(3):263–275. doi:10.1016/j.joes.2019.05.002.
Krishna MV, Chamkha AJ. Hall and ion slip effects on unsteady MHD convective rotating flow of nanofluids – application in biomedical engineering. J Egyptian Math Soc. 2020;28(1):1–14. doi:10.1186/s42787-019-0065-2.
Krishna MV. Heat transport on steady MHD flow of copper and alumina nanofluids past a stretching porous surface. Heat Transfer. 2020;49:1374–1385. doi:10.1002/htj.21667.
Krishna MV, Ahamad NA, Chamkha AJ. Hall and ion slip effects on unsteady MHD free convec- tive rotating flow through a saturated porous medium over an exponential accelerated plate. Alexandria Eng J. 2020;59:565–577. doi:10.1016/j.aej.2020.01.043.
Krishna MV, Sravanthi CS, Gorla RSR. Hall and ion slip effects on MHD rotating flow of ciliary propulsion of microscopic organism through porous media. Int Commun Heat Mass Transfer. 2020;112:104500. doi:10.1016/j.icheatmasstransfer.2020.104500.
Krishna MV, Chamkha AJ. Hall and ion slip effects on MHD rotating flow of elastico- viscous fluid through porous medium. Int Commun Heat Mass Transfer. 2020;113:104494. doi:10.1016/j.icheatmasstransfer.2020.104494.
Krishna MV. Hall and ion slip effects on MHD free convective rotating flow bounded by the semi- infinite vertical porous surface. Heat Transfer. 2020;49:1920–1938. doi:10.1002/htj.21700.